bioRxiv preprint doi: https://doi.org/10.1101/362194; this version posted July 4, 2018. The copyright holder for this preprint (which was not certified by peer review) is the author/funder, who has granted bioRxiv a license to display the preprint in perpetuity. It is made available under aCC-BY 4.0 International license.

The effect of anti-IL-6 receptor antibody for the treatment of McH-lpr/lpr-RA1 mice that spontaneously developed ankylosing arthritis

Takuya Izumiyama[1], Yu Mori[1]*, Kazu Takeda[2], Naoko Mori[3], Shiro Mori[2], Tetsuya Kodama[2], Eiji Itoi[1]

1: Department of Orthopaedic Surgery, Tohoku University Graduate School of Medicine

2: Laboratory of Biomedical Engineering for Cancer, Department of Biomedical Engineering, Graduate School of Biomedical Engineering, Tohoku University

3: Department of Diagnostic Radiology, Tohoku University Graduate School of Medicine

***Corresponding Author**: Yu Mori, Department of Orthopaedic Surgery, Tohoku University Graduate School of Medicine, 1-1 Seiryo-machi, Aoba-ku, Sendai, Miyagi 980-8574, Japan.

Tel: +81-22-717-7245; Fax: +81-22-717-7248; E-mail: yu-mori@med.tohoku.ac.jp

Takuya Izumiyama: takuya-izumiyama@med.tohoku.ac.jp

Yu Mori: yu-mori@med.tohoku.ac.jp

Kazu Takeda: kazutakeda@dc.tohoku.ac.jp

Naoko Mori: naokomori7127@gmail.com

Shiro Mori: shiromori@m.tohoku.ac.jp

Tetsuya Kodama: kodama@tohoku.ac.jp

Eiji Itoi: itoi-eiji@med.tohoku.ac.jp

Key words: Arthritis, Ankylosis, Anti-IL-6 receptor antibody, IVIS

bioRxiv preprint doi: https://doi.org/10.1101/362194; this version posted July 4, 2018. The copyright holder for this preprint (which was not certified by peer review) is the author/funder, who has granted bioRxiv a license to display the preprint in perpetuity. It is made available under aCC-BY 4.0 International license.

Abstract

[Background] McH-lpr/lpr-RA1 mice are a new strain of mice which spontaneously develop arthritis in the ankle, leading finally to ankylosis. There is no published data that drug treatment has been trialed on these mice.

[Objectives] This study examined the effect of the mouse anti-IL-6 receptor antibody, MR16-1, for the treatment of ankylosis in McH-lpr/lpr-RA1 mice.

[Methods] Male McH-lpr/lpr-RA1 mice were randomly divided into control and treatment groups. MR16-1 was administered from 10 weeks of age for the treatment group. Saline was applied for the control group. The drug was administered once a week, at an initial dose of 2 mg, then maintained at 0.5 mg once per week thereafter. The effects were evaluated by the histopathological synovitis score, in vivo imaging using indocyanine green liposomes, and analysis of the gene expression of inflammatory cytokines.

[Results] Tissue analyses were carried out at 14, 17 and 20 weeks of age. The synovitis scores of treated groups were significantly lower compared with those of the control group at every age. The kappa coefficient was 0.77. However, progression of ankylosis persisted in the MR16-1 treated group. In vivo imaging using indocyanine green liposomes showed significant decreases in signal intensities of treated groups at week 14, but no significant differences were observed at week 18. Blood serum amyloid A levels in treated groups were significantly lower at 17 weeks of age. The gene expression levels of *Tnf* and *Il17* were also significantly lower in MR16-1 treated groups.

[Conclusions] Administration of the anti-IL-6 receptor antibody is effective for the treatment of synovitis and bone destruction of McH-lpr/lpr-RA1 mice. McH-lpr/lpr-

bioRxiv preprint doi: https://doi.org/10.1101/362194; this version posted July 4, 2018. The copyright holder for this preprint (which was not certified by peer review) is the author/funder, who has granted bioRxiv a license to display the preprint in perpetuity. It is made available under aCC-BY 4.0 International license.

RA1 mice may be a suitable experimental model for the development of new treatments for spondyloarthritis. IL6 signal blockade could contribute to the treatment of spondyloarthritis, and further studies should be carried out to confirm its potential in the prevention of deformity associated with ankylosis.

Introduction

Spondyloarthritis diseases have complex pathological features, including synovitis, bone erosion, enthesitis and joint ankylosis [1]. The imbalance of bone and cartilage formation and the destruction of joint structure results in the structural changes observed in these diseases. Rheumatoid arthritis is characterized by synovial proliferation and erosion of joint cartilage due to chronic inflammation [2]. On the other hand, spondyloarthritis involves a distinct remodeling process leading to entheseal ossification and joint ankylosis, with synovial proliferation and bone erosion [3,4]. The histological characteristics of ankylosis include the proliferation of cartilage formation, and subsequent replacement of cartilage by bone (endochondral ossification) [5,6]. Recent studies have reported that IL-17 and IL-22 signaling molecules released from IL-23 positive T cells are involved in entheseal chondral proliferation and ossification [7,8]. Patients with ankylosing arthritis are typically treated with tumor necrosis factor (TNF)-α inhibitors. However, the prevention of ankylosis is recognized as being difficult especially in advanced stages of the disease [9-11]. Moreover, animal models of ankylosing arthritis are yet to be established. It is necessary to study animal models

bioRxiv preprint doi: https://doi.org/10.1101/362194; this version posted July 4, 2018. The copyright holder for this preprint (which was not certified by peer review) is the author/funder, who has granted bioRxiv a license to display the preprint in perpetuity. It is made available under aCC-BY 4.0 International license.

of ankylosing arthritis to elucidate the pathological mechanisms of the disease, and develop new treatment methods.

Our research group have previously reported the development of a murine model with spontaneous, progressive ankylosis in ankle joints [12]. Backcross generation mice were prepared using a non-arthritis strain of mice, C3H/HeJ-lpr/lpr (C3H/lpr), MRL/lpr × (MRL/lpr × C3H/lpr) F1. Among these N2 mice, we observed development of arthritis of the ankle joints, with macroscopic swelling. We then began to intercross the N2 mice, by selection based on swelling of the ankle joints. Finally, we established a novel recombinant strain of mice, designated McH-lpr/lpr-RA1, which showed a high incidence of arthritis with enthesopathy. Analysis of the joint remodeling processes may elucidate the fundamental mechanisms of spondyloarthritis and other ankylosing diseases.

The anti-IL-6 receptor monoclonal antibody is available for clinical use in patients with rheumatoid arthritis, and has been shown to have therapeutic effects in the treatment of severe rheumatoid arthritis [13]. The effect of anti-IL-6 treatment in patients with ankylosing spondylitis has also been reported — studies revealed that the anti-IL-6 receptor antibody did not prevent the progression of spinal changes associated with ankylosis [14]. Furthermore, the effect of treatment with anti-IL-6 receptor antibody on peripheral symptoms of spondyloarthritis has also been reported, but its use in joint ankylosis remains unclear [15]. MR16-1 is a rat anti-IL-6 receptor monoclonal antibody, as previously described in the literature [16]. MR16-1 is used in many experimental disease models to assess the effects of blocking IL-6 signaling [17-21]. McH-lpr/lpr-RA1 mice may provide a suitable animal model to assess the therapeutic

bioRxiv preprint doi: https://doi.org/10.1101/362194; this version posted July 4, 2018. The copyright holder for this preprint (which was not certified by peer review) is the author/funder, who has granted bioRxiv a license to display the preprint in perpetuity. It is made available under aCC-BY 4.0 International license.

94 effects of IL-6 signal blockade in ankylosing arthritis, and the administration of MR16-
95 1 will determine the potential treatment effects of IL-6 ligand and receptor blockade.
96 The purpose of the present study is to investigate the effect of MR16-1 for the treatment
97 of ankylosing arthritis, and the mechanism of inflammatory change and ankylosis in the
98 experimental murine model of McH-lpr/lpr-RA1 mice. We hypothesized that IL-6
99 signal blockade would suppress the progression of synovial proliferation and joint
100 ankylosis in McH-lpr/lpr-RA1 mice.
101
102 **Methods**
103 **Animals**
104 McH/lpr-RA1 mice were generated using F54 C3H/HeJ-*lpr/lpr* and MRL/lpr ×
105 (MRL/lpr × C3H/lpr) mice. This recombinant congenic strain of mice was designated
106 McH/lpr-RA1 as previously described in the literature [12]. All mice were housed in the
107 animal unit of Tohoku University Medical School, an environmentally controlled and
108 specific pathogen-free facility. Animal protocols were reviewed and approved by the
109 Tohoku University Animal Studies Committee. All experiments were performed using
110 week 10 male mice.
111 **Treatment of mice**
112 IL-6 signal blockade was performed with an intraperitoneal injection of 2 mg of rat anti-
113 mouse IL-6R mAb (MR16-1, a kind gift from Chugai Pharmaceutical, Tokyo, Japan),
114 once in the first treatment (week 10). Thereafter, 0.5 mg of MR 16-1 was administered
115 once a week until 20 weeks of age as previously described in the literature [22]
116 Phosphate buffered saline (PBS) was administered on the same schedule as a negative
117 control.

bioRxiv preprint doi: https://doi.org/10.1101/362194; this version posted July 4, 2018. The copyright holder for this preprint (which was not certified by peer review) is the author/funder, who has granted bioRxiv a license to display the preprint in perpetuity. It is made available under aCC-BY 4.0 International license.

Microcomputed tomography analysis

Microcomputed tomography (micro-CT) imaging was performed at 20 weeks of age (n=5 for each group). Harvested tibiae were stored in 70% ethanol at 4 °C, and analyzed using a micro-CT scanner (Scan Xmate-L090; Comscan Techno Co. Ltd., Kanagawa, Japan) operated at a peak voltage of 75 kV and 100 μA. The scanned region included 505 images from the proximal end of the tibia, at a resolution of 10.4 μm per voxel, and an image size of 516 × 506 pixels. Bone volume (BV; mm^2), total volume (TV; mm^2), bone volume fraction (BV/TV; %) and trabecular thickness (mm) were evaluated and calculated from the axial slice of the proximal tibia using TRI/3D-BON software (Ratoc System Engineering Co., Tokyo, Japan), as previously described in the literature [23].

Enzyme-linked immunosorbent assay

Serum amyloid A (SAA) and IL-6 levels were determined using an enzyme-linked immunosorbent assay (ELISA) kit for SAA and IL-6 (Biosource, Camarillo, CA and R&D Systems Inc., Minneapolis, MN, USA) according to the manufacturer's recommendations at 14 and 17 weeks of age (n=5 for each group). Briefly, serum samples were diluted 1:200 in assay diluent and incubated with conjugated anti-mouse SAA antibody. Serum samples were incubated with anti-mouse IL-6 antibody without dilution. Substrate tetramethylbenzidine was added, samples were read at OD450 nm and results were analyzed using the four-parameter fit to determine SAA values.

Histomorphometric analysis

Ankle joints were harvested at 14, 17 and 20 weeks of age and decalcified by soaking in 220 mM/L EDTA-Na for 3 weeks. Decalcified samples were sectioned and stained with hematoxylin and eosin for histopathological evaluation of synovitis and ankylosis, as

bioRxiv preprint doi: https://doi.org/10.1101/362194; this version posted July 4, 2018. The copyright holder for this preprint (which was not certified by peer review) is the author/funder, who has granted bioRxiv a license to display the preprint in perpetuity. It is made available under aCC-BY 4.0 International license.

previously described in the literature [24]. The calculated synovitis score was the sum of scores for: enlargement of the synovial lining cell layer (0 points: thickness of 1 layer; 1 point: thickness of 2-3 layers; 2 points: thickness of 4-5 layers; 3 points: thickness of more than 5 layers), density of the resident cells (0 points: normal cellularity; 1 point: slightly increased cellularity; 2 points: moderately increased cellularity; 3 points: greatly increased cellularity, pannus formation and rheumatoid like granulomas might occur) and inflammatory infiltrate (0 points: no inflammatory infiltrate; 1 point: few lymphocytes or plasma cells; 2 points: numerous lymphocytes or plasma cells, sometimes forming follicle-like aggregates; 3 points: dense, band-like inflammatory infiltrate, or numerous large, follicle-like aggregates). The synovitis score was assessed by two researchers and the kappa coefficient was calculated (n=5 for each group).

Synthesis of indocyanine green liposomes

Indocyanine green (ICG) liposomes were prepared as previously described in the literature [25-27]. Briefly, 1,2-distearoyl-sn-glycero-3-phosphatidylcholine (DSPC; NOF, Tokyo, Japan) and 1,2-distearoyl-sn-glycero-3-phosphoethanolamine-N-[methoxy-(polyethylene glycol)-2000] (DSPE-PEG[2000-OMe]) (DSPE-PEG:NOF, 94:6 mol/mol) were placed in a pear-shaped flask, and chloroform was added until the lipids were completely dissolved. The chloroform was then evaporated under reduced pressure using a rotary evaporator (NVC-2100/N-1000, Eyela, Tokyo, Japan) until a lipid film remained.

Next, 100 μM of ICG (Daiichi Sankyo, Tokyo, Japan) dissolved in 10 mL PBS was added to the thin lipid film to form multi-lamellar liposome vesicles. After repeated freeze-thaw cycles, the size of the liposomes was adjusted to <100 nm using extrusion

bioRxiv preprint doi: https://doi.org/10.1101/362194; this version posted July 4, 2018. The copyright holder for this preprint (which was not certified by peer review) is the author/funder, who has granted bioRxiv a license to display the preprint in perpetuity. It is made available under aCC-BY 4.0 International license.

166 equipment (Northern Lipids Inc., Vancouver, BC, Canada) with four filter sizes (100,
167 200, 400 and 600 nm; Nuclepore Track-Etch Membrane, Whatman plc, Maidstone,
168 UK). For sterilization, liposomes were passed through a 0.45 μm pore size filter (Millex
169 HV filter unit, Durapore polyvinylidene-difluoride [PVDF] membrane, EMD Millipore,
170 Billerica, MA, USA). Unbound ICG was removed using PD-10 columns. The lipid
171 concentration was measured using the Wako Phospholipids C test (Wako Pure
172 Chemical Industries, Osaka, Japan), and adjusted to 1.0 μmol/mL. Diameters of the ICG
173 liposomes were measured using a particle size analyzer (ELSZ-2,Otsuka Electronics,
174 Osaka, Japan).

175 **In vivo bioluminescence imaging system analysis**

176 In vivo bioluminescence imaging system (IVIS) analysis was performed at 10, 14 and
177 18 weeks of age in MR16-1 treated and control mice (n=5 for each group). Two
178 hundred milliliters of ICG liposomes was administered intravenously. The fluorescence
179 intensity of leaked ICG was measured at 0, 5, 30, 60, 120 and 180 minutes after
180 injection using an IVIS; Xenogen, Alameda, CA, USA), as previously described in the
181 literature [25,26].

182 **Quantitative RT-PCR**

183 Synovial tissue specimens from ankle joints were harvested at 10, 14 and 16 weeks of
184 age (n=5 for each group). Total RNA was extracted using QIAzol Lysis Reagent (Qiagen,
185 Hilden, Germany) and an RNeasy Mini Kit (Qiagen, Hilden, Germany). Synthesis of
186 cDNA from total RNA was carried out using RT buffer, RT random primers, dNTP mix,
187 and Multiscribe reverse transcriptase (Applied Biosystems, Foster city, CA, USA). A
188 total of 9 μL cDNA diluted 1:9 was added to 10 μL Taqman Universal Master Mix II
189 with Uracil N-glycosylase (Applied Biosystems, Foster City, CA, USA). Real-time

bioRxiv preprint doi: https://doi.org/10.1101/362194; this version posted July 4, 2018. The copyright holder for this preprint (which was not certified by peer review) is the author/funder, who has granted bioRxiv a license to display the preprint in perpetuity. It is made available under aCC-BY 4.0 International license.

amplification of the genes was performed using 1 µL ready-to-use Taqman Gene Expression Assays (Applied Biosystems) for *Il6*, *Tnf*, *IL17,* and *gapdh* as an endogenous control (assay IDs: Mm00446190_m1, Mm00443260_g1, Mm00439618_m1, and Mm99999915_g1). Relative gene expression data were analyzed using the delta-delta-Ct method with PCR-efficiency correction using StepOne software version 2.2.2 (Applied Biosystems), as previously described in the literature [28].

Statistical analysis

Statistical analyses were performed using JMP software version 13.1 (SAS, Cary, NC, USA). All data are expressed as the mean ± standard error (SE). Statistical significance of the differences between values were evaluated using the Student's t-test. Values of $p < 0.05$ were regarded as statistically significant. Kappa coefficients were calculated using SPSS version 21 (IBM, Armonk, NY, USA).

Results

Micro CT analysis

In the coronal-reconstructed micro CT images at 20 weeks of age, there were no apparent differences between MR16-1 treatment group and control group mice (Fig 1A). Quantitative structural analyses of proximal tibia are shown in Fig 1B. No significant differences were seen in BV, TV, BV/TV or trabecular thickness between the two groups. MR16-1 treatment therefore does not correlate with an increase in bone volume in McH/lpr-RA1 mice.

ELISA assay

The results of the ELISA assays showed reduced levels of SAA in the MR16-1 treatment group at 14 weeks of age, with significantly decreased levels at week 17 (p

bioRxiv preprint doi: https://doi.org/10.1101/362194; this version posted July 4, 2018. The copyright holder for this preprint (which was not certified by peer review) is the author/funder, who has granted bioRxiv a license to display the preprint in perpetuity. It is made available under aCC-BY 4.0 International license.

=0.0011) (Fig 2A). The results of the assay for serum IL-6 indicated no significant difference between the control and MR16-1 treatment groups at 14 and 17 weeks of age (Fig 2B).

Histomorphometric analysis

At 14 weeks of age, control group mice showed apparent synovitis, pannus formation, entheseal inflammation and ankylosis in the ankle region (Fig 3A and 3B). In MR16-1 treated mice, synovitis and pannus formation was suppressed compared with the control group (Fig 3C and 3D). At 17 weeks of age, control group mice exhibited acceleration of synovitis, pannus formation and ankle joint ankylosis (Fig 4A and 4B). In the MR16-1 treatment group, no synovitis or pannus formation were detected, however, the progression of entheseal ankylosis was seen (Fig 4C and 4D). At 20 weeks of age, control group mice showed degenerative synovial lesions, advanced pannus formation and ankylosing change (Fig 5A and 5B). In the MR16-1 treatment group, ossification and ankylosis of the entheseal area was found, although synovitis and pannus formation were absent (Fig 5C and 5D). Histopathological assessments of ankle arthritis were performed by calculation of the synovitis score. The Kappa coefficient was calculated to be 0.77, and the reproducibility was good. At week 14, the synovitis score of the control group was 4.29 ± 019, and that of the MR16-1 group was 2.75 ± 0.53. This indicates a significant difference between the two groups ($p = 0.0036$). At week 17, the synovitis score of the control group was 3.95 ± 0.22, and that of the MR16-1 group was 1.64 ± 0.27. This indicates a significant difference between the two groups ($p < 0.001$). At week 20, the synovitis score of the control group was 3.33 ± 0.28, and that of the MR16-1 group was 2.25 ± 0.3. This indicates a significant difference between the two groups ($p = 0.0125$) (Fig 6).

bioRxiv preprint doi: https://doi.org/10.1101/362194; this version posted July 4, 2018. The copyright holder for this preprint (which was not certified by peer review) is the author/funder, who has granted bioRxiv a license to display the preprint in perpetuity. It is made available under aCC-BY 4.0 International license.

238 **IVIS analysis**

239 The changes in the signal intensities pre-injection and 120 minutes after injection were
240 assessed. Representative images of 14 weeks of age control mice and MR16-1 treated
241 mice are shown in Fig 7A and 7B. MR16-1 treated mice did not show ICG
242 accumulation in the ankle or foot joints. However, control mice showed obvious
243 accumulation in the foot and ankle joints. The results of IVIS analyses are shown in Fig
244 8. Quantitative IVIS was carried out at weeks 10, 14 and 18 in control and MR16-1
245 treated mice. There was a significant difference in the signal intensities of control and
246 MR16-1 treated mice at week 14 ($p=0.0003$), although there no significant differences
247 were seen at weeks 10 or 18.

248 **Quantitative RT-PCR**

249 The results of quantitative PCR analyses are shown in Fig 9. *Tnf* gene expression
250 gradually decreased until week 16 in the MR16-1 treatment group. There was a
251 significant difference in *Tnf* gene expression between the two groups at week 16
252 ($p=0.004$), which was lower in the MR16-1 treated group than the control group. *Il17*
253 gene expression also gradually decreased until week 16 in the MR16-1 treatment group.
254 There were also significant differences in *Il17* gene expression between the two groups
255 at week 14 and 16 ($p=0.044$; $p=0.042$), which were lower in MR16-1 treated group. *Il6*
256 gene expression was also evaluated, revealing no significant difference in expression
257 levels between the groups.

258

259 **Discussion**

260 Previous studies have reported several murine models that develop spontaneous
261 ankylosis [29]. For example, DBA/1 mice spontaneously develop ankylosing

bioRxiv preprint doi: https://doi.org/10.1101/362194; this version posted July 4, 2018. The copyright holder for this preprint (which was not certified by peer review) is the author/funder, who has granted bioRxiv a license to display the preprint in perpetuity. It is made available under aCC-BY 4.0 International license.

arthropathy in the ankle joints [30-32]. However, these mice mainly exhibit fibrous proliferation in enthesis and fibrous ankylosis, without erosion and bone destruction [29]. McH/lpr-RA1 mice show synovitis, pannus formation and ankylosis, resembling spondyloarthritis [12]. We consider that McH/lpr-RA1 mice are a suitable experimental disease model of spondyloarthritis. The present study explores the effects of treatment with the anti-IL-6 receptor monoclonal antibody in McH/lpr-RA1 mice. In the MR16-1 treated group, results of histomorphometric and IVIS analyses showed that the proliferation of synovium and joint destruction were suppressed. However, histological investigations confirmed that ankylosis progressed even with IL-6 blockade treatment. We propose that the anti-IL-6 receptor antibody contributes to the suppression of synovial proliferation in McH/lpr-RA1 mice, but that further factors are involved in the prevention of entheseal ankylosis.

Changes in the bone parameters of MR16-1 treated and control mice were evaluated by micro-CT imaging. In this study there were no significant differences in the bone parameters between two groups. A published study reported the treatment effects of MR16-1 to include increased bone volume in DBA/1 mice [33]. However, in this study McH/lpr-RA1 mice did not show increased bone volume following MR16-1 treatment. In the published study, the dose of MR16-1 was much higher — 8 mg was administered to DBA/1 mice. Our different findings of the effect of MR16-1 treatment on bone volume were likely due to the different dosage of MR16-1.

SAA was significantly lower in the MR16-1 treated group, and we consider that the dose of MR16-1 that was administered is sufficient to suppress inflammation in McH/lpr-RA1 mice. MR16-1 is an anti-IL-6 receptor antibody for the treatment, so it is unsurprising that there were no changes in serum IL-6 level. The results of quantitative

bioRxiv preprint doi: https://doi.org/10.1101/362194; this version posted July 4, 2018. The copyright holder for this preprint (which was not certified by peer review) is the author/funder, who has granted bioRxiv a license to display the preprint in perpetuity. It is made available under aCC-BY 4.0 International license.

RT-PCR showed that gene expression levels of *tnf* and *IL17* were suppressed by IL-6 signal blockade. Previous studies reported that IL-6 signal blockade by MR16-1 suppresses IL-17 signaling [34,35]. Suppression of IL-6, TNF- α and IL-17 signals may contribute to the prevention of synovitis and bone destruction in McH/lpr-RA1 mice. However, only partial prevention of joint ankylosis was seen in the MR16-1 treated group — at week 20 the histological images showed the progression of ankylosis, regardless of the prevention of synovial proliferation and bone destruction. In the results of previous clinical trials, administration of anti-IL-6 receptor antibody was insufficient for complete treatment of ankylosing spondylitis [14]. Some studies have reported that entheseal ankylosis in spondyloarthritis is related to IL-17 signaling [36]. The blockade of IL-17 signaling was achieved in this study; however, this signal suppression might be insufficient, as other signaling pathways (such as IL-12, IL-22 and IL-23) could be involved in the mechanisms of entheseal ossification and ankylosis. Our results are consistent with the results of human clinical trials of anti-IL-6 receptor antibody treatment in ankylosing spondylitis. We consider that McH/lpr-RA1 is an adequate animal model of spondyloarthritis, and a promising tool for the evaluation and development of new treatment reagents and drug repositioning treatment in spondyloarthritis.

The results of IVIS analyses showed that there was a significant difference between the two groups in week 14 only. These results are inconsistent with the results of histological analyses, PCR and ELISA of SAA, which indicated significant differences after week 14. We consider that spontaneous arthritis in McH/lpr-RA1 mice becomes self-limiting around week 18. The histological findings showed significant differences in late phase arthritis, including bone erosion, pannus formation and ankylosis.

bioRxiv preprint doi: https://doi.org/10.1101/362194; this version posted July 4, 2018. The copyright holder for this preprint (which was not certified by peer review) is the author/funder, who has granted bioRxiv a license to display the preprint in perpetuity. It is made available under aCC-BY 4.0 International license.

However, IVIS analyses did not indicate significant differences in late phase arthritis due to self-limitation of inflammation in the joints.

Conclusion

In the present study, we have demonstrated for the first time that IL-6 signal blockade with MR16-1 significantly reduces the development of synovitis and joint destruction in the murine experimental model of spondyloarthritis, McH/lpr-RA1. Our results indicate that the progression of deformity associated with ankylosis continues even with anti-IL-6 receptor antibody treatment; indicating that further factors might be involved in the progression of joint ankylosis. McH/lpr-RA1 is a promising animal model for the elucidation of the mechanism of spondyloarthropathy and development of new treatment.

Abbreviations

BV: Bone volume

CT: Computed tomography

cDNA: complementary DNA

ELISA: Enzyme-linked immunosorbent assay

ICG: Indocyanine green

IL: Interleukin

IVIS: In vivo bioluminescence imaging system

PBS: Phosphate-buffered saline

RT-PCR: Realtime polymerase chain reaction

SAA: Serum amyloid A

bioRxiv preprint doi: https://doi.org/10.1101/362194; this version posted July 4, 2018. The copyright holder for this preprint (which was not certified by peer review) is the author/funder, who has granted bioRxiv a license to display the preprint in perpetuity. It is made available under aCC-BY 4.0 International license.

334 **TNF:** Tumor necrosis factor

335 **TV:** Total volume

336

337 **Declarations**

338 ***Acknowledgements***

339 This study was supported by JSPS KAKENHI (18K09052) URL of Japan Society for
340 the Promotion of Science is as follows: https://www.jsps.go.jp/english./index.html. The
341 funders had no role in study design, data collection and analysis, decision to publish, or
342 preparation of the manuscript.

343 ***Author's Contributions***

344 Conceived and designed the experiments: TI, YM, SM, TK.

345 Performed the experiments: TI, YM, KT.

346 Contributed materials/analysis tools: YM, SM, TK

347 Wrote the manuscript: TI, YM, NM, EI

348 ***Ethics approval***

349 Experiments were approved by The Tohoku University Animal Studies Ethics
350 Committee.

351 ***Competing interests***

352 The authors have declared that no competing interests exist.

353 **References**

354 1. Ronneberger M, Schett G. Pathophysiology of Spondyloarthritis. Current
355 Rheumatology Reports. 2011;13:416–20.

356 2. Scott DL, Wolfe F, Huizinga TW. Rheumatoid arthritis. 2010;376:15.

bioRxiv preprint doi: https://doi.org/10.1101/362194; this version posted July 4, 2018. The copyright holder for this preprint (which was not certified by peer review) is the author/funder, who has granted bioRxiv a license to display the preprint in perpetuity. It is made available under aCC-BY 4.0 International license.

357 3. BENJAMIN M, McGONAGLE D. The anatomical basis for disease localisation in
358 seronegative spondyloarthropathy at entheses and related sites. J Anat. 2001;199:503–
359 26.
360 4. Paramarta JE, van der Leij C, Gofita I, Yeremenko N, van de Sande MG, de Hair MJ,
361 et al. Peripheral joint inflammation in early onset spondyloarthritis is not specifically
362 related to enthesitis. Annals of the Rheumatic Diseases. 2014;73:735–40.
363 5. Lories RJU, Matthys P, Vlam K de, Derese I, Luyten FP. Ankylosing enthesitis,
364 dactylitis, and onychoperiostitis in male DBA/1 mice: a model of psoriatic arthritis. Ann
365 Rheum Dis. 2004;63:595–8.
366 6. Oishi H, Miyazaki T, Mizuki S, Kamogawa J, Lu L-M, Tsubaki T, et al. Accelerating
367 effect of an MRL gene locus on the severity and onset of arthropathy in DBA/1 mice.
368 Arthritis & Rheumatism. 52:959–66.
369 7. Reinhardt A, Yevsa T, Worbs T, Lienenklaus S, Sandrock I, Oberdörfer L, et al.
370 Interleukin-23–Dependent γ/δ T Cells Produce Interleukin-17 and Accumulate in the
371 Enthesis, Aortic Valve, and Ciliary Body in Mice. Arthritis & Rheumatology. 68:2476–
372 86.
373 8. Sherlock JP, Joyce-Shaikh B, Turner SP, Chao C-C, Sathe M, Grein J, et al. IL-23
374 induces spondyloarthropathy by acting on ROR-γt+ CD3+CD4−CD8− entheseal
375 resident T cells. Nature Medicine. 2012;18:1069–76.
376 9. Baraliakos X, Heldmann F, Callhoff J, Listing J, Appelboom T, Brandt J, et al.
377 Which spinal lesions are associated with new bone formation in patients with
378 ankylosing spondylitis treated with anti-TNF agents? A long-term observational study
379 using MRI and conventional radiography. Annals of the Rheumatic Diseases.
380 2014;73:1819–25.

bioRxiv preprint doi: https://doi.org/10.1101/362194; this version posted July 4, 2018. The copyright holder for this preprint (which was not certified by peer review) is the author/funder, who has granted bioRxiv a license to display the preprint in perpetuity. It is made available under aCC-BY 4.0 International license.

381 10. Weiß A, Song I-H, Haibel H, Listing J, Sieper J. Good correlation between changes
382 in objective and subjective signs of inflammation in patients with short- but not long
383 duration of axial spondyloarthritis treated with tumor necrosis factor-blockers. Arthritis
384 Research & Therapy. 2014;16:R35.
385 11. Zhang J-R, Liu X-J, Xu W-D, Dai S-M. Effects of tumor necrosis factor-α inhibitors
386 on new bone formation in ankylosing spondylitis. Joint Bone Spine. 2016;83:257–64.
387 12. Mori S, Tanda N, Ito MR, Oishi H, Tsubaki T, Komori H, et al. Novel recombinant
388 congenic mouse strain developing arthritis with enthesopathy. Pathology International.
389 2008;58:407–14.
390 13. Teitsma XM, Marijnissen AKA, Bijlsma JWJ, Lafeber FPJ, Jacobs JWG.
391 Tocilizumab as monotherapy or combination therapy for treating active rheumatoid
392 arthritis: a meta-analysis of efficacy and safety reported in randomized controlled trials.
393 Arthritis Research & Therapy. 2016;18(1):211.
394 14. Sieper J, Porter-Brown B, Thompson L, Harari O, Dougados M. Assessment of
395 short-term symptomatic efficacy of tocilizumab in ankylosing spondylitis: results of
396 randomised, placebo-controlled trials. Ann Rheum Dis. 2014;73:95–100.
397 15. Lekpa F, Poulain C, Wendling D, Soubrier M, De Bandt M, Berthelot J, et al. Is IL-
398 6 an appropriate target to treat spondyloarthritis patients refractory to anti-TNF therapy?
399 a multicentre retrospective observational study. Arthritis Research & Therapy.
400 2012;14:R53.
401 16. Mihara, Takagi, Takeda, Ohsugi. IL-6 receptor blockage inhibits the onset of
402 autoimmune kidney disease in NZB/W F1 mice. Clinical & Experimental Immunology.
403 112:397–402.

bioRxiv preprint doi: https://doi.org/10.1101/362194; this version posted July 4, 2018. The copyright holder for this preprint (which was not certified by peer review) is the author/funder, who has granted bioRxiv a license to display the preprint in perpetuity. It is made available under aCC-BY 4.0 International license.

404 17. Arima H, Hanada M, Hayasaka T, Masaki N, Omura T, Xu D, et al. Blockade of IL-
405 6 signaling by MR16-1 inhibits reduction of docosahexaenoic acid-containing
406 phosphatidylcholine levels in a mouse model of spinal cord injury. Neuroscience.
407 2014;269:1–10.
408 18. Birner P, Heider S, Petzelbauer P, Wolf P, Kornauth C, Kuroll M, et al.
409 Interleukin-6 receptor alpha blockade improves skin lesions in a murine model of
410 systemic lupus erythematosus. Exp Dermatol. 2016;25:305–10.
411 19. Iwanami K, Matsumoto I, Tanaka-Watanabe Y, Inoue A, Mihara M, Ohsugi Y, et
412 al. Crucial role of the interleukin-6/interleukin-17 cytokine axis in the induction of
413 arthritis by glucose-6-phosphate isomerase. Arthritis & Rheumatism. 58:754–63.
414 20. Ohtsuji M, Lin Q, Nishikawa K, Ohtsuji N, Okazaki H, Tsurui H, et al. IL-6 signal
415 blockade ameliorates the enhanced osteoclastogenesis and the associated joint
416 destruction in a novel FcγRIIB-deficient rheumatoid arthritis mouse model. Modern
417 Rheumatology. 2015;25:270–7.
418 21. Suzuki M, Yoshida H, Hashizume M, Tanaka K, Matsumoto Y. Blockade of
419 interleukin-6 receptor enhances the anti-arthritic effect of glucocorticoids without
420 decreasing bone mineral density in mice with collagen-induced arthritis. Clin Exp
421 Immunol. 2015;182:154–61.
422 22. Yoshida H, Hashizume M, Suzuki M, Mihara M. Induction of high-dose tolerance
423 to the rat anti-mouse IL-6 receptor antibody in NZB/NZW F1 mice. Rheumatology
424 International. 2011;31:1445–9.
425 23. Kamimura M, Mori Y, Sugahara-Tobinai A, Takai T, Itoi E. Impaired Fracture
426 Healing Caused by Deficiency of the Immunoreceptor Adaptor Protein DAP12. PLoS
427 One. 2015; doi:10.1371/journal.pone.0128210.

bioRxiv preprint doi: https://doi.org/10.1101/362194; this version posted July 4, 2018. The copyright holder for this preprint (which was not certified by peer review) is the author/funder, who has granted bioRxiv a license to display the preprint in perpetuity. It is made available under aCC-BY 4.0 International license.

428 24. Krenn V, Morawietz L, Burmester G-R, Kinne RW, Mueller-Ladner U, Muller B, et
429 al. Synovitis score: discrimination between chronic low-grade and high-grade synovitis.
430 Histopathology. 2006;49:358–64.
431 25. Kato S, Mori S, Kodama T. A Novel Treatment Method for Lymph Node Metastasis
432 Using a Lymphatic Drug Delivery System with Nano/Microbubbles and Ultrasound.
433 Journal of Cancer. 2015;6:1282–94.
434 26. Mikada M, Sukhbaatar A, Miura Y, Horie S, Sakamoto M, Mori S, et al. Evaluation
435 of the enhanced permeability and retention effect in the early stages of lymph node
436 metastasis. Cancer Science. 2017;108:846–52.
437 27. Kodama T, Tomita N, Horie S, Sax N, Iwasaki H, Suzuki R, et al. Morphological
438 study of acoustic liposomes using transmission electron microscopy. Journal of Electron
439 Microscopy. 2010;59:187–96.
440 28. Fujisawa H, Mori Y, Kogure A, Tanaka H, Kamimura M, Masahashi N, et al.
441 Effects of intramedullary nails composed of a new β-type Ti-Nb-Sn alloy with low
442 Young's modulus on fracture healing in mouse tibiae.J Biomed Mater Res B Appl
443 Biometer. 2018; doi:10.1002/jbm.b.34064.
444 29. Breban M, Araujo LM, Chiocchia G. Editorial: Animal Models of
445 Spondyloarthritis: Do They Faithfully Mirror Human Disease? Arthritis &
446 Rheumatology. 66:1689–92.
447 30. Holmdahl R, Jansson L, Andersson M, Jonsson R. Genetic, hormonal and
448 behavioural influence on spontaneously developing arthritis in normal mice. Clin Exp
449 Immunol. 1992;88:467–72.

bioRxiv preprint doi: https://doi.org/10.1101/362194; this version posted July 4, 2018. The copyright holder for this preprint (which was not certified by peer review) is the author/funder, who has granted bioRxiv a license to display the preprint in perpetuity. It is made available under aCC-BY 4.0 International license.

450 31. Nordling C, Karlsson-Parra A, Jansson L, Holmdahl R, Klareskog L.
451 Characterization of a spontaneously occurring arthritis in male DBA/1 mice. Arthritis &
452 Rheumatism. 1992;35:717–722.
453 32. Weinreich S, Capkova J, Hoebe-Hewryk B, Boog C, Ivanyi P. Grouped caging
454 predisposes male mice to ankylosing enthesopathy. Ann Rheum Dis. 1996;55:645–7.
455 33. Tanaka K, Hashizume M, Mihara M, Yoshida H, Suzuki M, Matsumoto Y. Anti-
456 interleukin-6 receptor antibody prevents systemic bone mass loss via reducing the
457 number of osteoclast precursors in bone marrow in a collagen-induced arthritis model:
458 Anti-IL-6R antibody prevents systemic bone mass loss. Clinical & Experimental
459 Immunology. 2014;175:172–80.
460 34. Hashimoto-Kataoka T, Hosen N, Sonobe T, Arita Y, Yasui T, Masaki T, et al.
461 Interleukin-6/interleukin-21 signaling axis is critical in the pathogenesis of pulmonary
462 arterial hypertension. Proceedings of the National Academy of Sciences.
463 2015;112:E2677–86.
464 35. Hirota K, Hashimoto M, Yoshitomi H, Tanaka S, Nomura T, Yamaguchi T, et al. T
465 cell self-reactivity forms a cytokine milieu for spontaneous development of IL-17+ Th
466 cells that cause autoimmune arthritis. J Exp Med. 2007;204:41–7.
467 36. Speeckaert R, van Geel N, Lambert J, Claeys L, Delanghe JR, Speeckaert MM.
468 Secukinumab: IL-17A inhibition to treat psoriatic arthritis. Drugs of Today.
469 2016;52:607.

470

471 **Figure Legends**

472 **Figure 1. Micro CT image of tibia at week 20 in control and MR16-1 treated**
473 **groups**

bioRxiv preprint doi: https://doi.org/10.1101/362194; this version posted July 4, 2018. The copyright holder for this preprint (which was not certified by peer review) is the author/funder, who has granted bioRxiv a license to display the preprint in perpetuity. It is made available under aCC-BY 4.0 International license.

(A) Representative coronal reconstruction images of proximal tibia in control and MR16-1 treated groups.

(B) Structural parameter analyses of tibia of control and MR16-1 treated mice. There are no significant differences in BV, TV, BV/TV and trabecular thickness.

Figure 2. ELISA assays for SAA and IL-6

(A) ELISA assay for SAA at week 14 and 17. Serum SAA level is significantly lower in MR16-1 treated group at week 17.

(B) ELISA assay for IL-6 at week 14 and 17. There is no significant difference in serum IL-6 level.

Figure 3. Histological images of control and MR16-1 treated groups at week 14

Representative histological images of ankle joint and foot in control group. (A) is ×40 lower magnification image. (B) is ×100 higher magnification image. Rectangle shows the higher magnification area. Arrows indicate synovial proliferation. * indicates entheseal fibrous and cartilaginous ankylosis.

Representative histological images of ankle joint and foot in MR16-1 treatment group. (C) is ×40 lower magnification image. (D) is ×100 higher magnification image. Rectangle shows the higher magnification area. Arrows indicate synovial proliferation. * indicates fibrous and cartilaginous ankylosis.

Figure 4. Histological images of control and MR16-1 treated groups at week 17

Representative histological images of ankle joint and foot in control group. (A) is ×40 lower magnification image. (B) is ×100 higher magnification image. Rectangle shows the higher magnification area. Arrows indicate synovial proliferation. * indicates entheseal fibrous and cartilaginous ankylosis.

bioRxiv preprint doi: https://doi.org/10.1101/362194; this version posted July 4, 2018. The copyright holder for this preprint (which was not certified by peer review) is the author/funder, who has granted bioRxiv a license to display the preprint in perpetuity. It is made available under aCC-BY 4.0 International license.

Representative histological images of ankle joint and foot in MR16-1 treatment group. (C) is ×40 lower magnification image. (D) is ×100 higher magnification image. Rectangle shows the higher magnification area. Arrows indicate synovial proliferation. * indicates entheseal fibrous and cartilaginous ankylosis.

Figure 5. Histological images of control and MR16-1 treated groups at week 20

Representative histological images of ankle joint and foot in control group. (A) is ×40 lower magnification image. (B) is ×100 higher magnification image. Rectangle shows the higher magnification area. Arrow heads indicate subsequent interosseous ankylosis after synovial proliferation. * indicates entheseal fibrous and cartilaginous ankylosis. Representative histological images of ankle joint and foot in MR16-1 treatment group. (C) is ×40 lower magnification image. (D) is ×100 higher magnification image. Rectangle shows the higher magnification area. * indicates entheseal fibrous and cartilaginous ankylosis.

Figure 6. Histomorphometric analyses with the synovitis grading score of foot and ankle joints in control and MR16-1 treated mice

The synovitis grading scores of MR16-1 treatment group are significantly lower in week 14, 17 and 20 compared with those of control group. * < 0.05, ** < 0.01, *** < 0.001.

Figure 7. IVIS analyses in control and MR16-1 treated mice

(A) Representative image of IVIS of control mouse at week 14. There are evident signals in both ankles and foots.

(B) Representative image of IVIS of MR16-1 treated mouse at week 14. There is no significant uptake signals in ankles and foots.

Figure 8. Quantitative analyses of signal intensity of IVIS at week 10, 14, 18

bioRxiv preprint doi: https://doi.org/10.1101/362194; this version posted July 4, 2018. The copyright holder for this preprint (which was not certified by peer review) is the author/funder, who has granted bioRxiv a license to display the preprint in perpetuity. It is made available under aCC-BY 4.0 International license.

521 At week 14, the signal intensity of IVIS of ankles and foots is significantly lower in
522 MR16-1 treatment group, compared with the control group. There are no significant
523 changes in week 10 and 18 in both groups. ** $p < 0.01$

524 **Figure 9. mRNA expression of *Tnf*, *Il17* and *Il6* genes**

525 The expression levels of *Tnf* is significantly lower in MR16-1 treated group at week 16.
526 The expression levels of *Il17* is significantly lower in MR16-1 treated group at week 14
527 and 16. There is no significant difference of *Il6* expression among both groups. *$p <$
528 0.05, ***$p < 0.001$

(A)

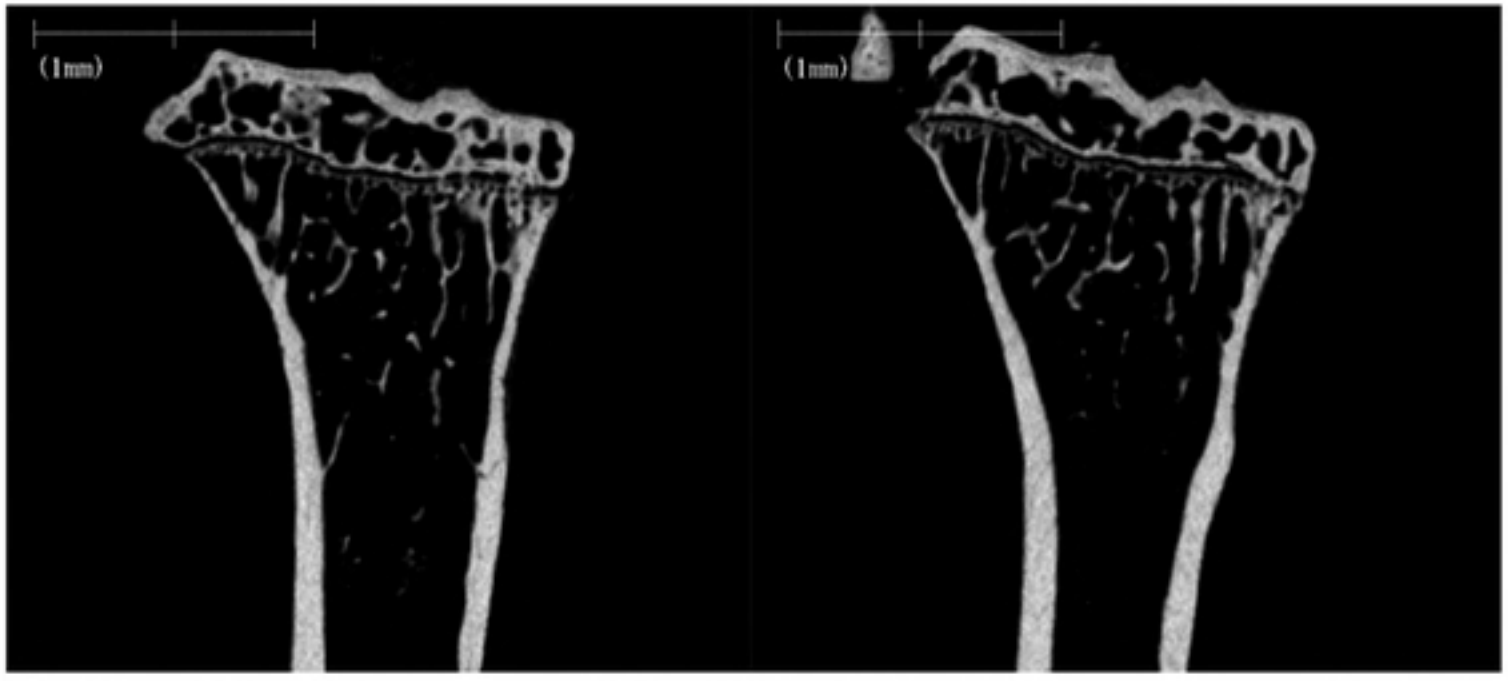
control
MR16−1
(1mm)
(1mm)

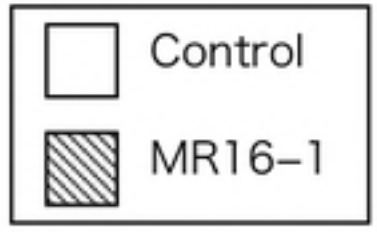
Control
MR16−1

(B)

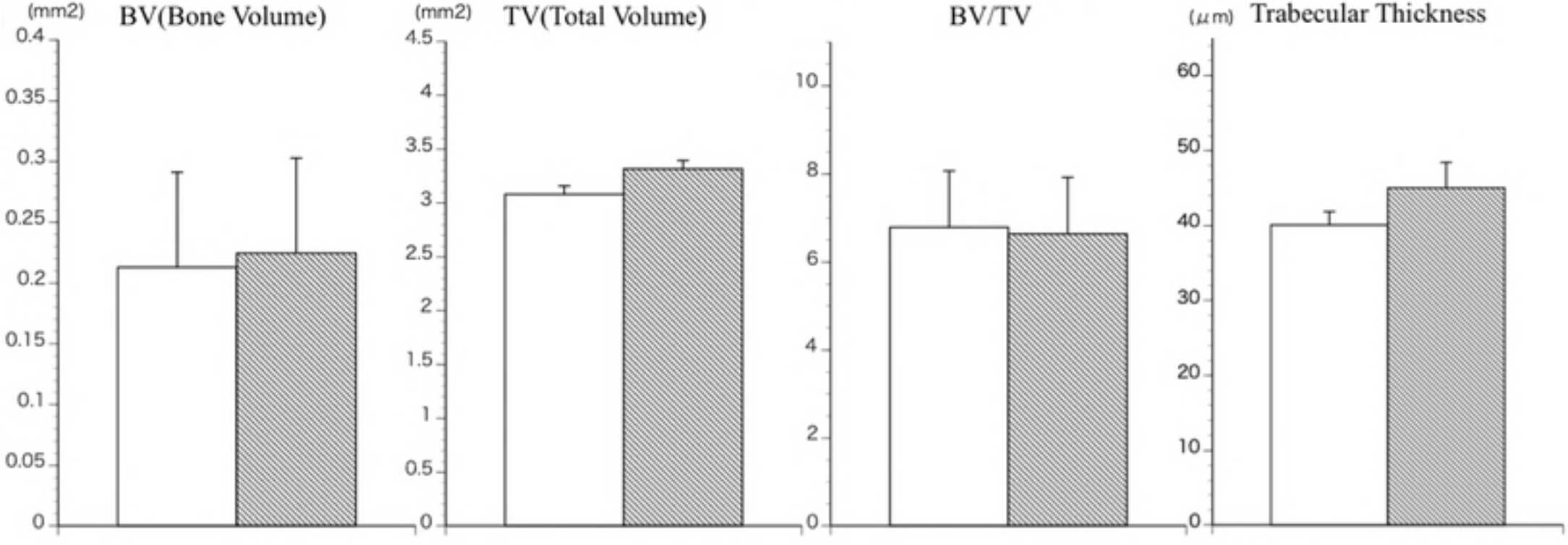
(mm2)
BV(Bone Volume)
0.4
0.35
0.3
0.25
0.2
0.15
0.1
0.05
0
(mm2)
TV(Total Volume)
4.5
4
3.5
3
2.5
2
1.5
1
0.5
0
BV/TV
10
8
6
4
2
0
(μm)
Trabecular Thickness
60
50
40
30
20
10
0

bioRxiv preprint doi: https://doi.org/10.1101/362194; this version posted July 4, 2018. The copyright holder for this preprint (which was not certified by peer review) is the author/funder, who has granted bioRxiv a license to display the preprint in perpetuity. It is made available under aCC-BY 4.0 International license.

(A)

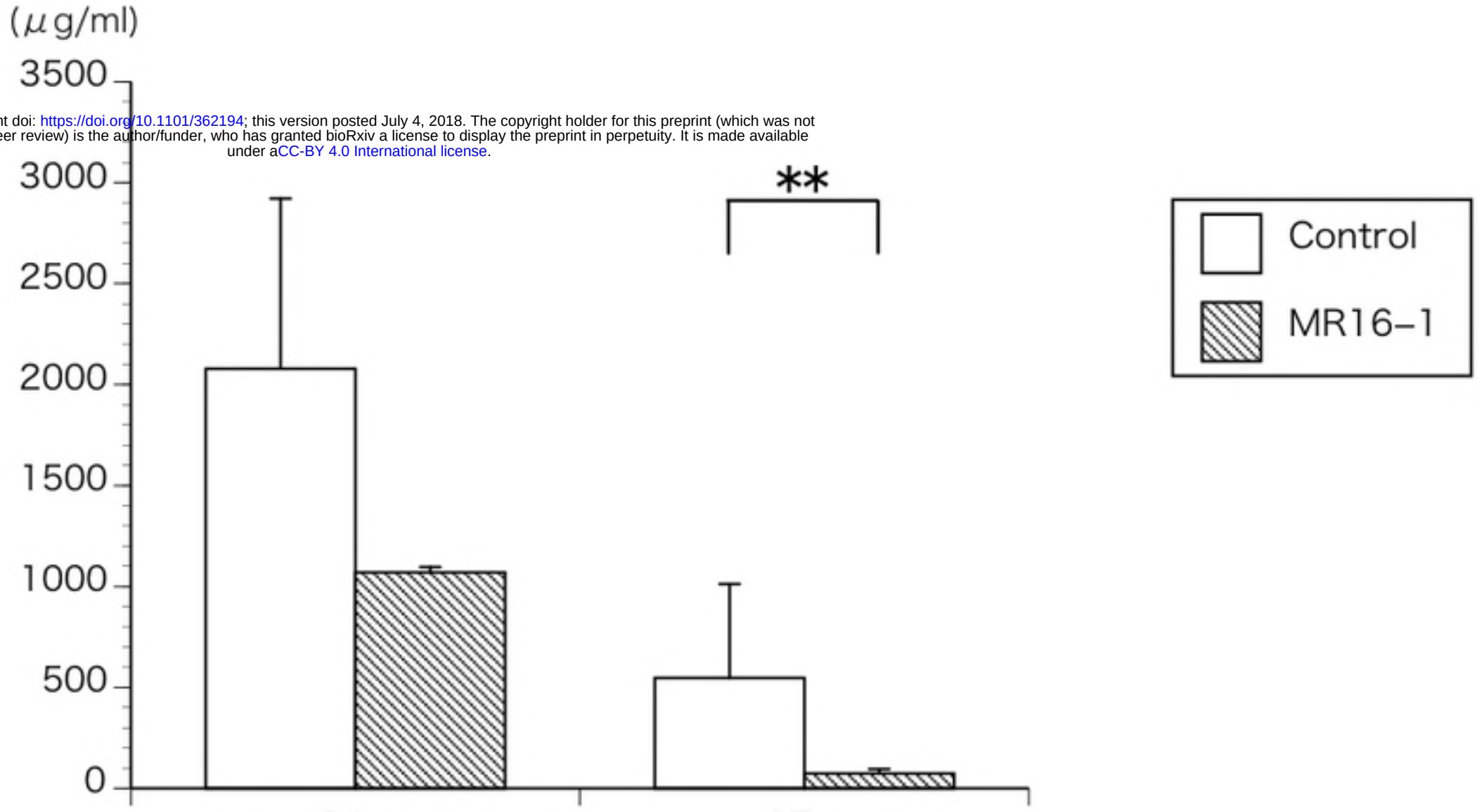

(B)

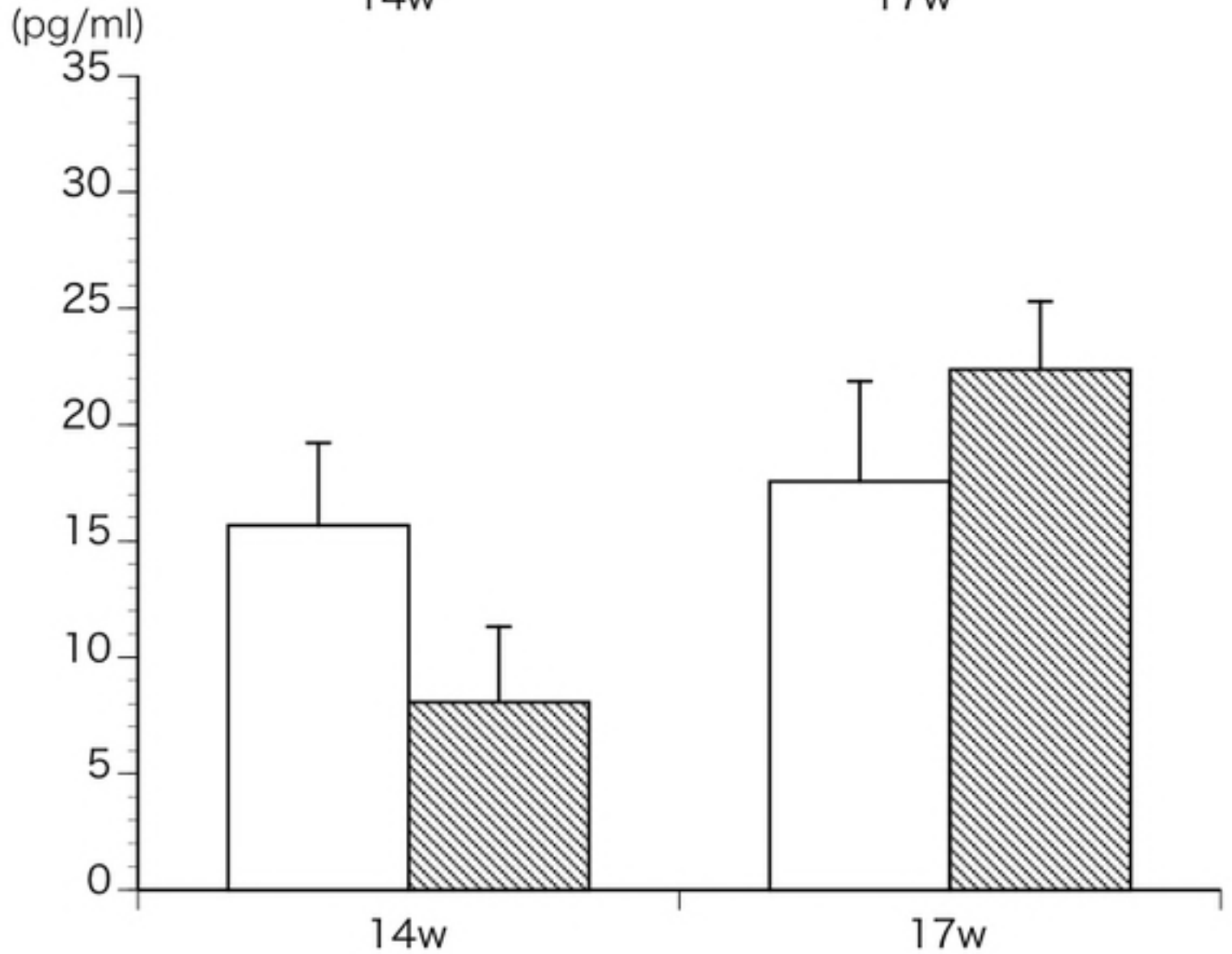

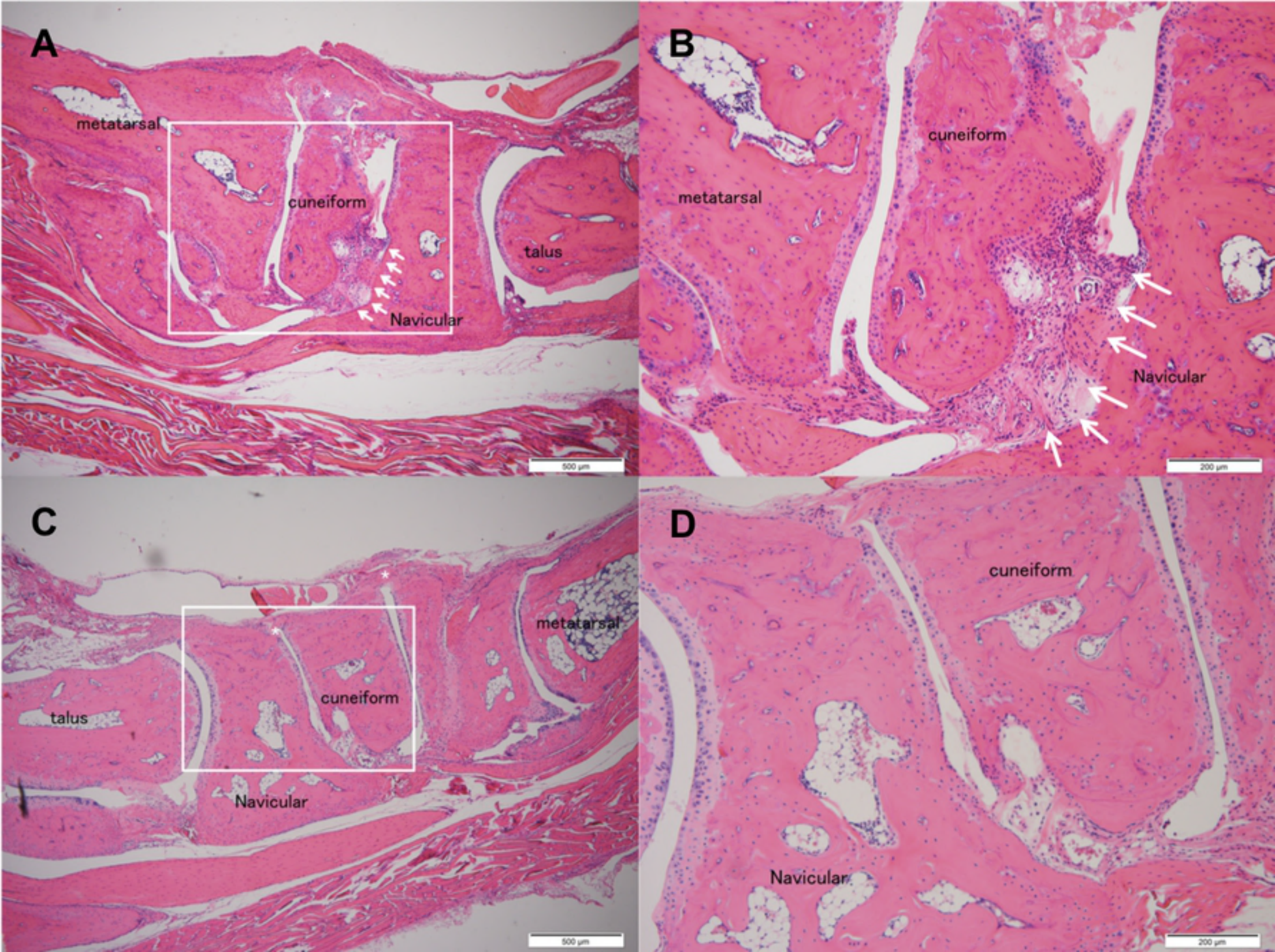
A
metatarsal
cuneiform
talus
Navicular
500 μm
B
cuneiform
metatarsal
Navicular
200 μm
C
metatarsal
cuneiform
talus
Navicular
500 μm
D
cuneiform
Navicular
200 μm

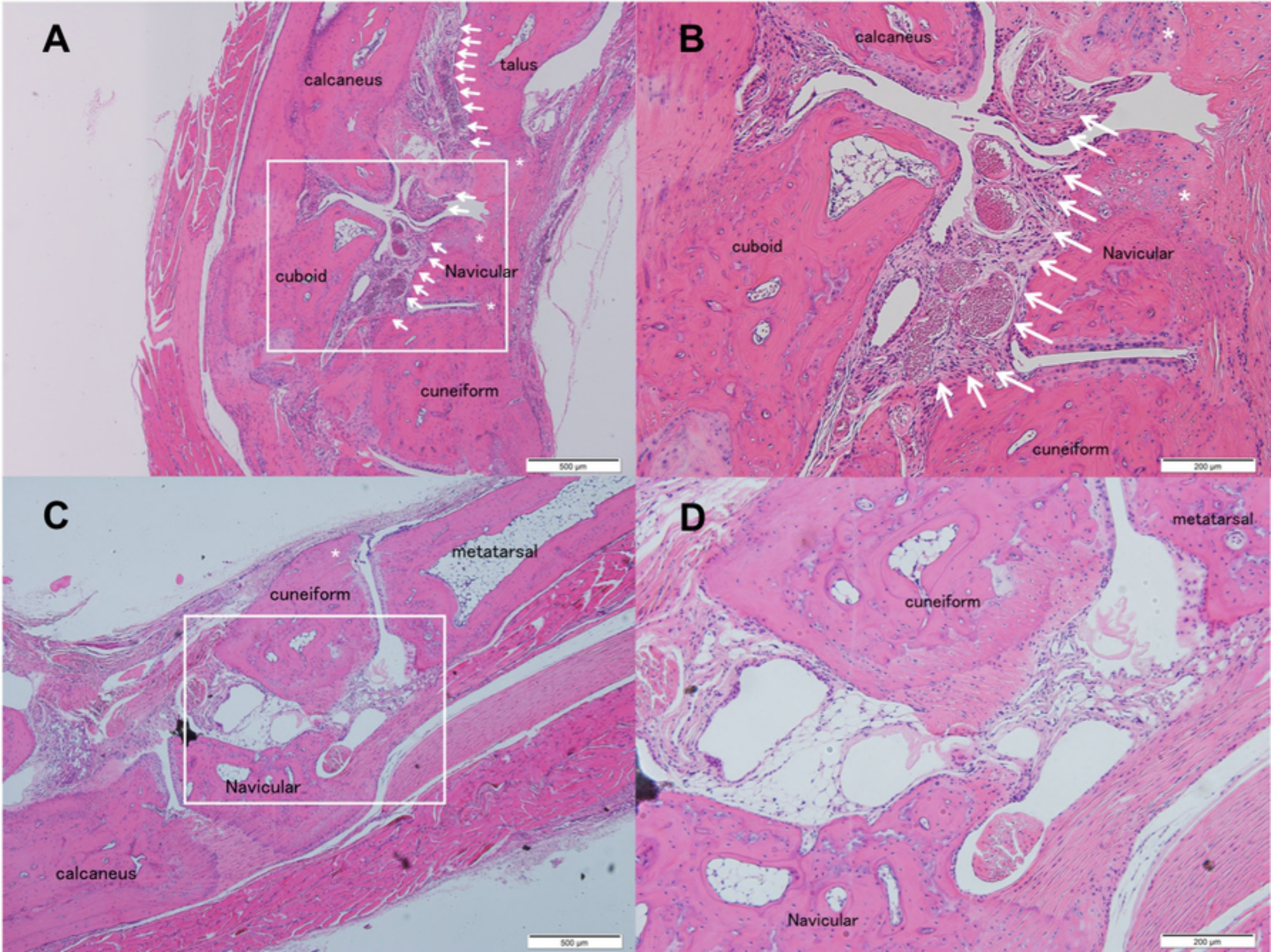
A
calcaneus
talus
cuboid
Navicular
cuneiform
500 μm
B
calcaneus
cuboid
Navicular
cuneiform
200 μm
C
metatarsal
cuneiform
Navicular
calcaneus
500 μm
D
metatarsal
cuneiform
Navicular
200 μm

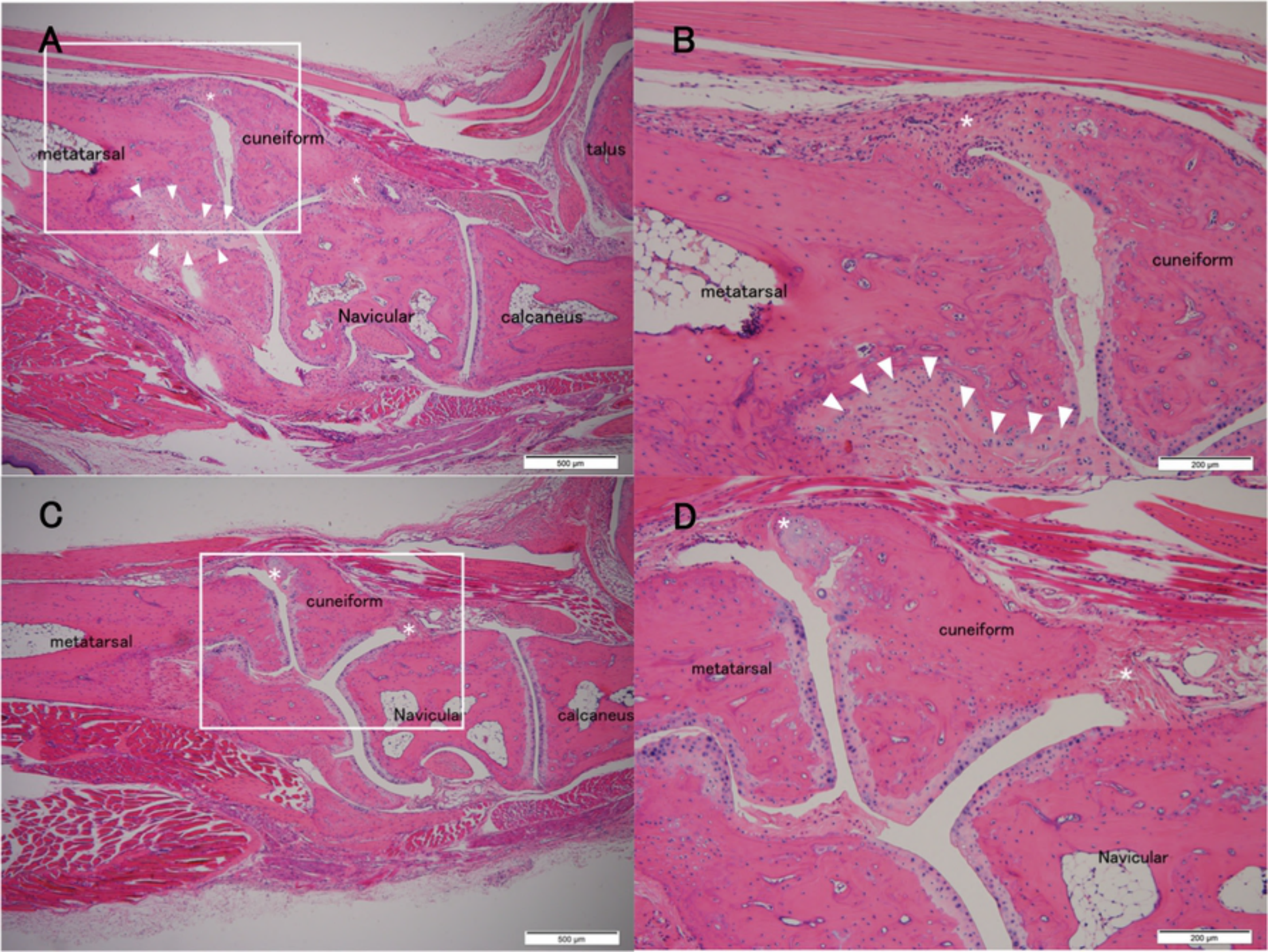
A
metatarsal
cuneiform
talus
Navicular
calcaneus
500 μm
B
metatarsal
cuneiform
200 μm
C
cuneiform
metatarsal
Navicula
calcaneus
500 μm
D
cuneiform
metatarsal
Navicular
200 μm

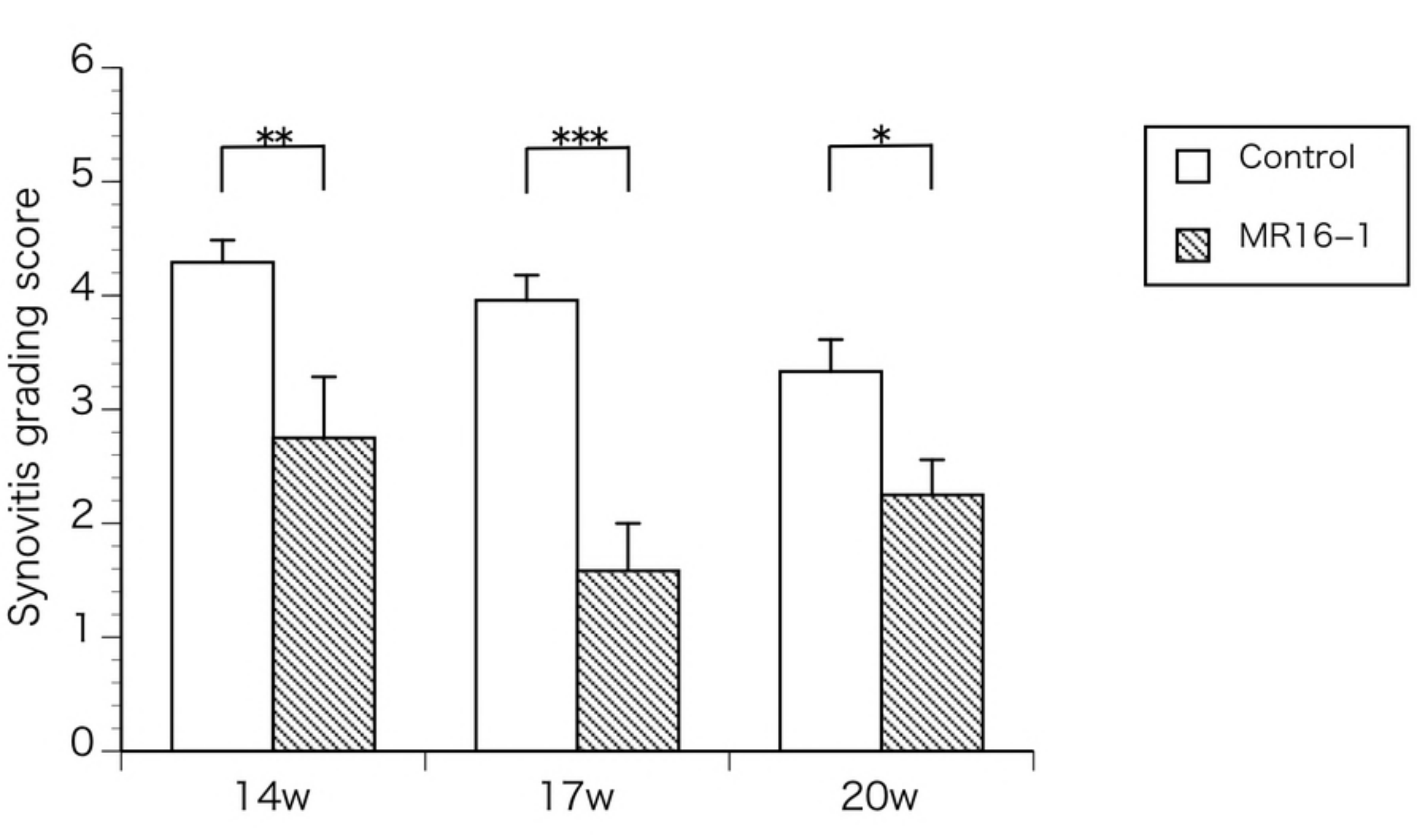
Synovitis grading score
6
5
4
3
2
1
0
**
***
*
14w
17w
20w
Control
MR16-1

(A)

(B)

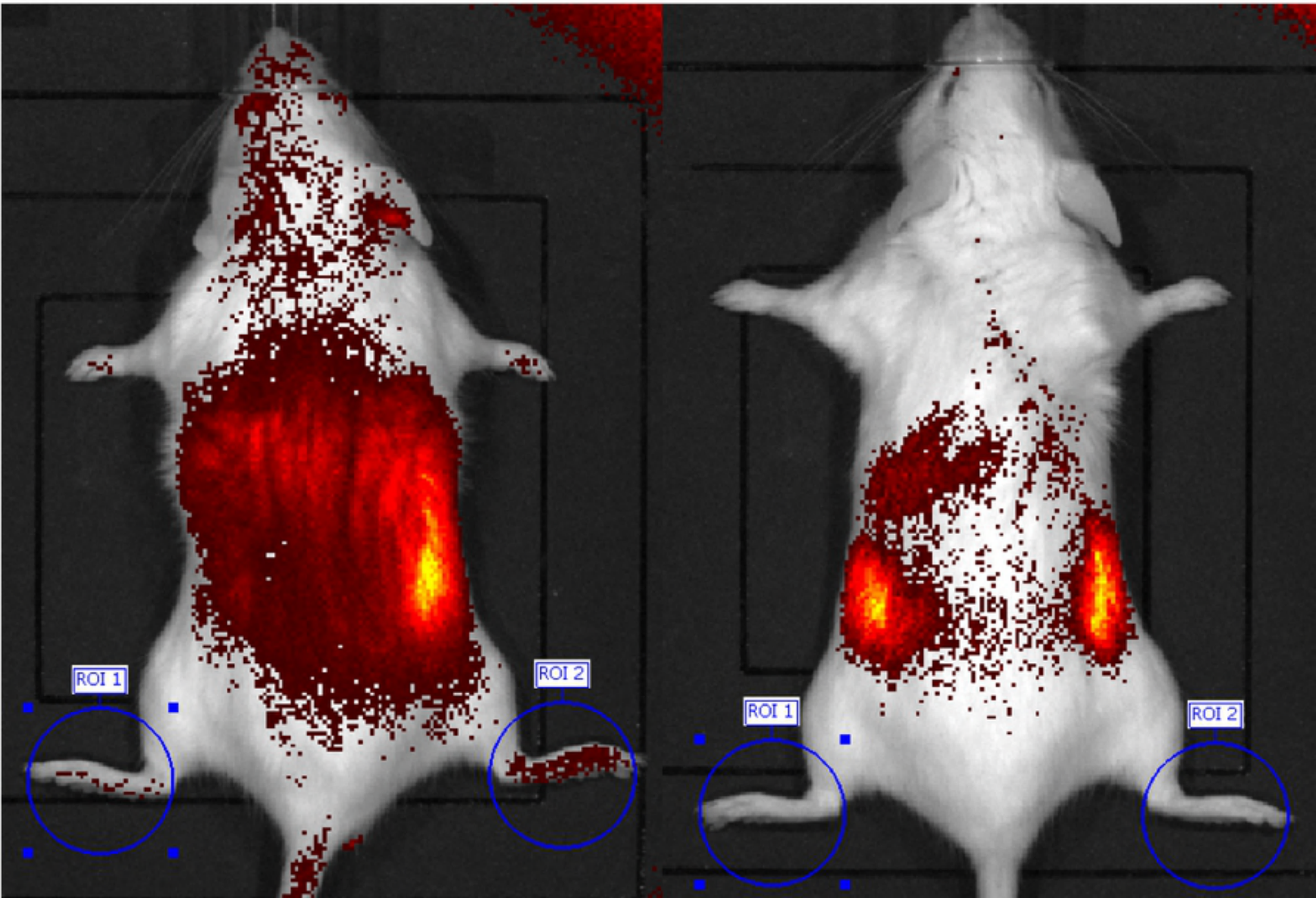

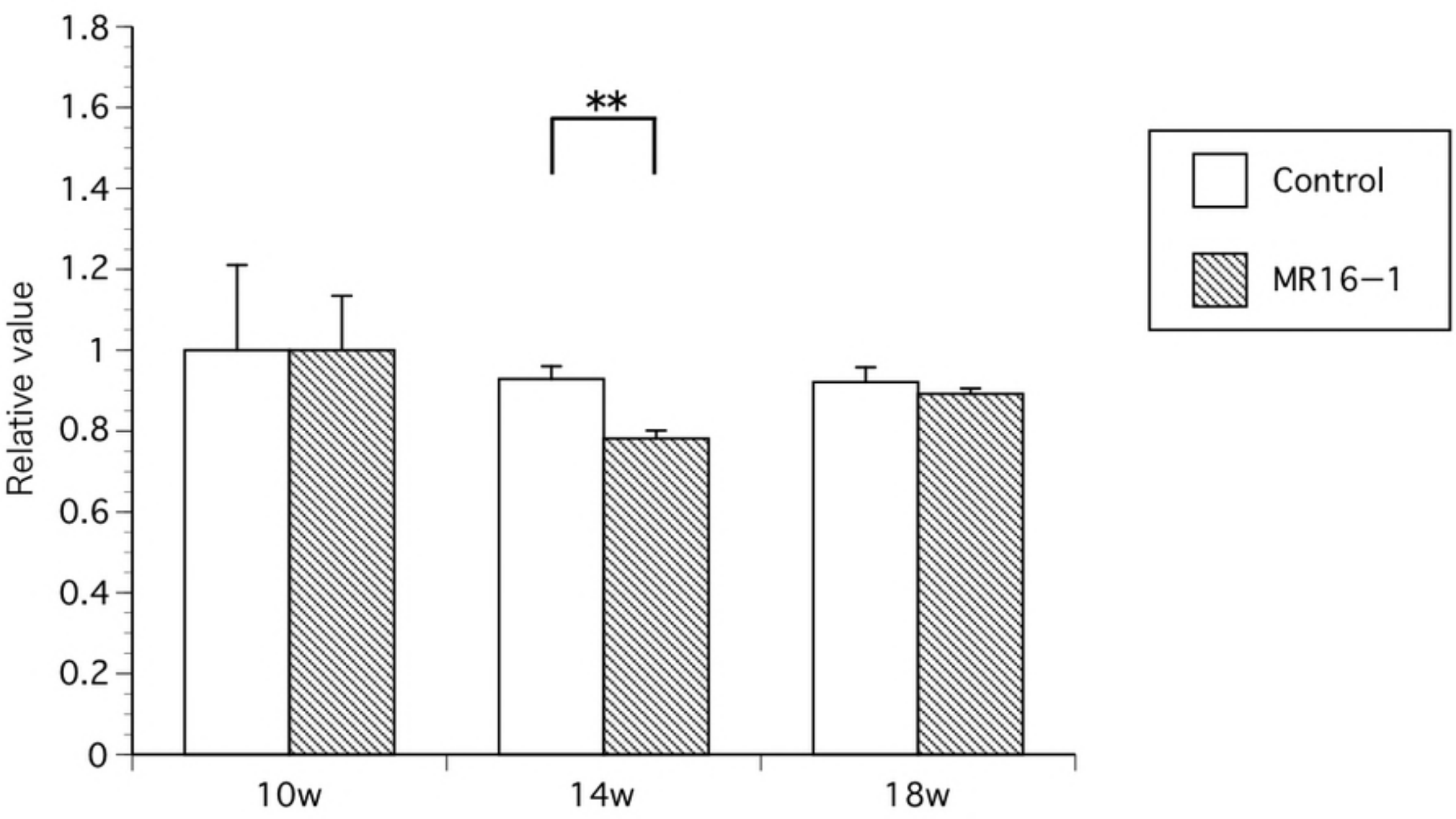
1.8
1.6
1.4
1.2
1
0.8
0.6
0.4
0.2
0
Relative value
**
Control
MR16−1
10w
14w
18w

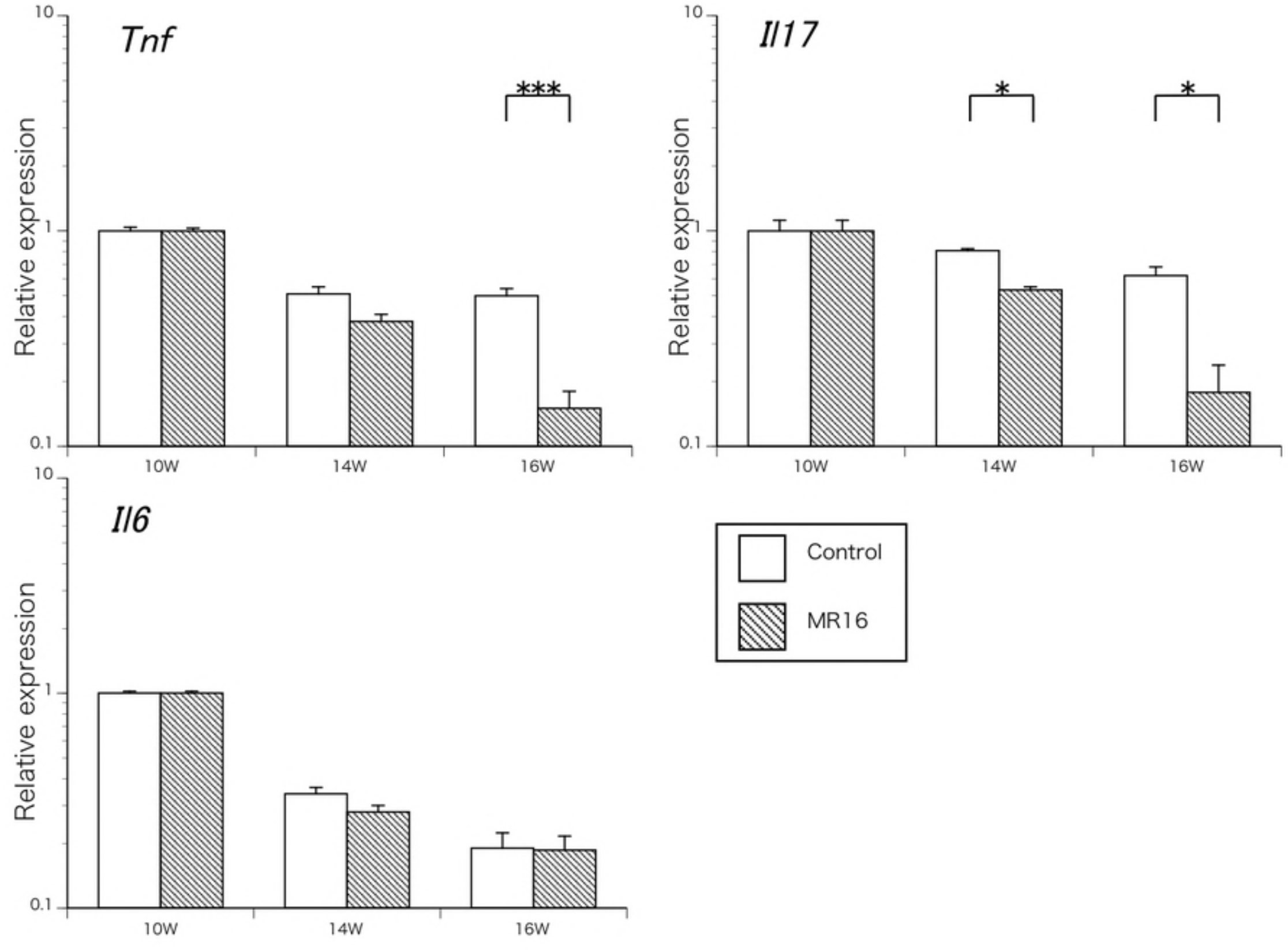
Tnf
Il17
Il6
Relative expression
10
1
0.1
10W
14W
16W
***
*
*
Control
MR16